System Monitoring and Prototype Drift Chamber Analysis Development for HELIX

Undergraduate Research Thesis

Presented in Partial Fulfillment of the Requirements for graduation "with Honors Research Distinction in Physics" at The Ohio State University

Richard Mueller

The Ohio State University

2020

Project Advisor: Jim Beatty, Department of Physics

Abstract

The High-Energy Light Isotope eXperiment (HELIX) was proposed to better constrain today's leading theoretical models of the structure of the universe, to which end it will specifically make high-statistics measurements of the $^{10}Be/^{9}Be$ isotopic ratio at high energies. Discussed here are the implementation of a monitoring system for several subsystems as well as analysis development for its prototype drift chamber (PDCT). The monitoring system, or housekeeping, was built to weather subsystem glitches, and its software implementation is discussed in detail. This network of sensors and subsystems was successfully tested by collecting over two days of data from HELIX's superconducting magnet subsystem. Analysis routines were applied to PDCT data with the goal of generalizing these tools directly to the soon-to-be-finished tracker. Algorithms were created to isolate cosmic ray muon events, whose drift times were statistically analyzed.

Acknowledgements

I would like to thank Prof. Jim Beatty for the opportunity to learn and work in his lab. I would also like to thank Keith McBride and Dr. Patrick Allison, who have been instrumental in helping me complete this project.

Table of Contents

Table of Figures

1. Cosmic Rays

1.1. Particle Astrophysics

Particle astrophysics is a field overlapping particle physics and cosmology. One primary goal of this study is understanding the nature and structure of matter in the universe. Direct measurements of cosmic rays, or high-energy particles that traverse the galaxy, aid this ambition. Cosmic rays constantly shower down to Earth, some originating in the sun and others from outside the solar system in supernovae or their remnants [1]. These measurements help in detailing information on the conditions of extreme objects in the galaxy, such as supernova. Local to the galaxy, cosmic ray measurements probe properties of the near empty space between stars systems, called the Interstellar Medium (ISM). Existing models of the Galaxy largely rely on specific cosmic ray measurements, such as secondary-to-primary ratios and isotopic abundance ratios, to identify their origins and detail their travels [2-5].

1.2. Secondary-to-primary Ratios

Cosmic ray composition and spectra are divided into nuclei that are directly created in cosmic ray sources (primaries) and nuclei that are produced by spallation—naturally occurring scattering that causes nucleosynthesis—of primaries in the ISM (secondaries). The secondary-to-primary ratio is the proportion of abundance of a primary against one of the secondary species it produces. These groups are not exclusive, and the flux of some nuclei at Earth are found in comparable amounts of both. Secondary cosmic rays are subject to the same processes which accelerate their primary counterparts, and just as well, are likely to lose energy. At low to medium energies it becomes difficult to attribute a population of a species as primary or secondary. However, at high-energies, primary cosmic rays are only found as elements which are stellar-nuclides (like H, He, C, N, O, Si, Fe) since no other species are created in stars (like Li, Be, Ne, etc.). Accordingly, higher-energy measurements are important in understanding cosmic ray histories.

Because the longer a cosmic ray travels the more likely it is to interact with the ISM, the secondary-to-primary ratio gives information about the propagation path of cosmic rays, and so their origin, as well as the structure of the ISM. Some astrophysical models, such as diffusion models with halos, are sensitive to a large number of parameters where another measurement, the isotopic abundance ratio, becomes of equal or greater importance [13-15].

1.3. Isotopic Abundance Ratios

Secondary cosmic rays in the form of radioactive isotopes provide an opportunity to study the universe on the timescales of which these species decay. The ratio of two isotopes of the same species, the isotopic abundance ratio, acts as a 'clock' if the isotope's lifetime is that of the timescale being investigated. The lifetime of a clock acts to resolve probable regions of origin. One such clock is ^{10}Be/^{9}Be. Because Be is produced in spallation in the ISM (as opposed to stellar nucleosynthesis), the ^{10}Be/^{9}Be ratio is entirely determined by the propagation history of cosmic rays. Higher-energy measurements can extend the domain of propagation model history, since the Lorentz boost lengthens half-lives. Furthermore, high-quality and high-statistics measurements of ^{10}Be/^{9}Be can be shown to discriminate between cosmic ray propagation models with opposing structural principles [6-8].

1.4. HELIX

In light of the importance of such measurements, the High-Energy Light Isotopy eXperiment (HELIX) was proposed to specifically make high-statistics measurements of the $^{10}Be/^{9}Be$ isotopic ratio at high energies. It will also take a measurement of the $^{3}He/^{4}He$ isotopic ratio, as well as the first measurements of $^{22}Ne/^{20}Ne$, $^{7}Li/^{6}Li$, and $^{10}B/^{11}Be$ above 1 GeV/n. The project employs a mass spectrometer to gather measurements at such high energies. In HELIX's mass spectrometer, a particle's momentum is determined by its speed and bending radius in the presence of a magnetic field. Specifically, the spectrometer consists of a 1 T superconducting magnet, a gas particle tracker, and an aerogel ring imaging Cherenkov (RICH) detector.

Since Ohio State joined the project in 2018, the OSU team has been involved in making a number of strategic improvements to the project. One responsibility of Ohio State was to implement and test the housekeeping system, which monitors a large number of sensors on the instrument to ensure working condition. Examples of which are pressure sensors on the gondola and temperatures of sensitive electronics. Additionally, the time-based data analysis of a prototype particle tracker was taken on by OSU. Below, the design of these projects and my role in their fulfillment is discussed.

2. The Housekeeping System

2.1. Purpose

The housekeeping system is a monitoring scheme designed to survey the status of some subsystems and confirm that operating conditions are within our expectations. For example, the temperature of many points around the payload are measured to a high precision to assist in diagnosing and explaining malfunctions. Solar panels and batteries that are the power source of many of the system's electronics are also closely monitored. The system acquires and relays data from many subsystems which are not directly related to HELIX's scientific mission but are needed for its success.

2.2. Design

Data acquisition for the housekeeping system is designed around a common architecture. One main housekeeping board controls several subsystems with the same protocol. These subsystems are designated to groups of sensors which are accessed through commands issued by the main housekeeping board. Communication with subsystem microcontrollers for configuration and measurement takes place on the same bus, requiring flexible software.

In this structure, information relay takes the form of several linked development boards sharing a serial communication system. Data collected from a sensor is sent down a stream of electronics to the main housekeeping board, which collects and repackages this information to be sent to HELIX's main computer, the science flight computer (SFC). The core of the main housekeeping board's software and most basic functions are common in each subsystem.

2.3. Integration with other Electronics

Ultimately the housekeeping system is beholden to the SFC. While the main housekeeping board is responsible for routine data collection, the SFC tells the main board which data to collect with pre-defined commands. The housekeeping system only manages the data it receives for a short period of time before sending it to the SFC for long term storage. Should an error occur somewhere in the housekeeping system the main board will relay the instance to the SFC, which contains a protocol for handling the system's errors, including performing a system reset. Specifically, the housekeeping system collects data from the drift chamber, 1 T magnet, gondola, and solar arrays which power the payload.

3. Particle Drift Chamber Trackers

As identifying cosmic ray species is central to HELIX's purpose, the project requires instrumentation to determine a particle's mass and charge. To determine mass, the project employs a drift chamber tracker.

3.1. Drift Chamber Basics

Drift chambers are used to determine the trajectory of a particle as it passes through. The drift chamber on HELIX is within a strong magnetic field. The effect of the magnetic field on a particle, the magnetic rigidity, is the actual quantity measured with this setup. Rigidity is given by $R = pc/Ze$ [with $p = \beta\gamma mc$ momentum, c is speed of light, and Ze is the electric charge]. Finding the rigidity, provided with separate measurements of the particle's charge Ze and velocity β, gives a value for mass m.

HELIX's drift chamber tracker is a box of pressurized, uniform gas containing thin metal wires spanning its length. Spanning wires, along with chamber walls, are placed with strategic voltage levels such that the electric field is near uniform from wall to wall. After adding a magnetic field, charged particles moving through the chamber will follow a curved arc.

The radius of curvature is only applicable for charged particle: a particle with charge Ze moving with relativistic velocity $\vec{p}/m$ through a uniform magnetic field $\vec{B}$ experiences $\frac{Ze}{m}\ \vec{p} \times \vec{B}$. This is equal to the centripetal force. Force balancing gives an expression for the mass of the particle in terms of the bending radius r:

$$R = B \cdot r = \frac{c^2}{Ze} m\,\gamma\beta$$

$$m = \frac{ZeBr}{c^2\,\gamma\,\beta}$$

3.2. Working Principle

When a charged particle moves through gas, it will strip electrons from the molecules it encounters, creating electron/ion pairs. These charged particle's move along electric field lines in their respective directions, causing more interactions with the gas and more ionization. The movement of electrons produces a time-based signal from which we can estimate the total time the electron traveled before interacting significantly with the gas, the drift time. Accurate knowledge of an electron's velocity within the chamber, its drift velocity, allows us to estimate the electron's starting radius from the sense wire (anode). This is the distance of closest approach (probabilistically) of the energetic charged

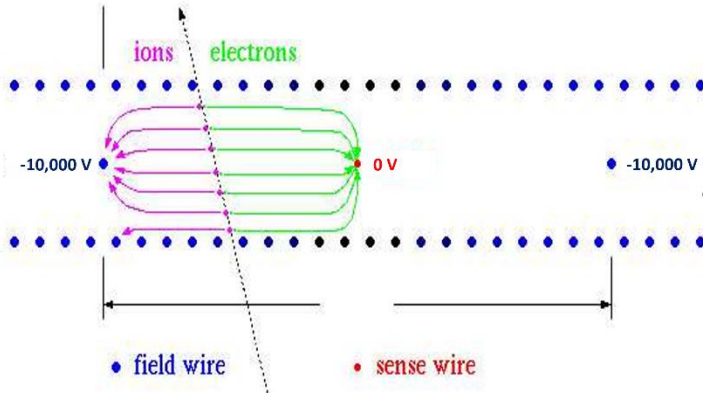

Figure 3.1: A particle traversing a drift chamber in the absence of a magnetic field, ionizing the surrounding gas. Electrons drift towards the sense wire, ions towards the anode. [12]

particle passing through the chamber. We reconstruct the trajectory of the charged particle by connecting many of these radii measurements.

3.2.1. Primary Gas Ionization

A drift chamber tracks a particle by identifying the position of consecutive sources of gas ionization. When high-energy charged particles travel through the gas, they probabilistically ionize gas molecules. In the PDCT, omni-directional cosmic ray muons produce

$$\mu^- \rightarrow \mu^- + e^- + CO_2^+$$

The freed electrons travel towards the anode, and ions (although much more slowly because of their size) towards the cathode.

3.2.2. Drift of Electrons

Electrons in a uniform electric field will quickly reach terminal velocity before approaching the anode [9]. Their drift velocity thus remains relatively stable as long as the time an electron spends in the uniform region of the electric field is much larger than the time it spends in the non-uniform region. Exact drift velocity depends on exact electric field strength E and gas pressure P.

3.2.3. Secondary Gas Ionization: Proportional Gas Gain

As the electron travels, it further ionizes the surrounding gas:

$$e^- + A \rightarrow e^- + A^+ + e^-, \text{ or } e^- + A^{++} + e^- + e^-, \text{ etc...}$$

The result is an 'avalanche' of electrons which collectively travels towards the (relatively) positive electrode of the electric field. The gain in ionization of the gas is described by the Townsend coefficient $\alpha(E)$, which is proportional to the 'gas gain' along an element of radial pathlength ds by

$$dN = N\,\alpha(E)ds$$

In large monotonic electric fields, the number of stripped electrons per unit distance (dN/ds) is roughly constant [9]. In our case, the region where we can make this assumption is confined to the space far enough from the wire for the field to be approximately constant. Typically, dN/ds is found by shooting a beam of known particle's through the box and measuring the signal.

3.2.4. Signal Creation

In the simplest case of signal induction by moving charges in the drift chamber, a free charge e travels towards a single anode, or sense wire. This induces a time-dependent charge on the wire, meaning a current of

$$I(t) = \frac{4we}{\pi(4\,z_0(t)^2 + w^2)}v$$

where $z_0(t)$ is the particle's radial position from a wire of width w, traveling at speed v [9]. Hence, once an electron reaches a sense wire, the signal ends. Also note that because ions travel longer, they produce the majority of work on the sense wires, albeit the signal lasts orders of magnitude longer because of their slower drift velocity. By making the anodes sensitive to fast current signals, we can measure an analogue signal proportional to the number of electrons.

3.3. Prototype Chamber Overview

The prototype drift chamber is an 8.5 x 8.5 x 18 cm rectangular box containing a single layer of staggered sense wires. The cathodes (walls) of the chamber are kept at -10,000 V, and in regions far from the eight grounded sense wires, the electric field is constant. Because the electric field is not changing, the electrons quickly reach peak drift velocity and move at this speed in this region.

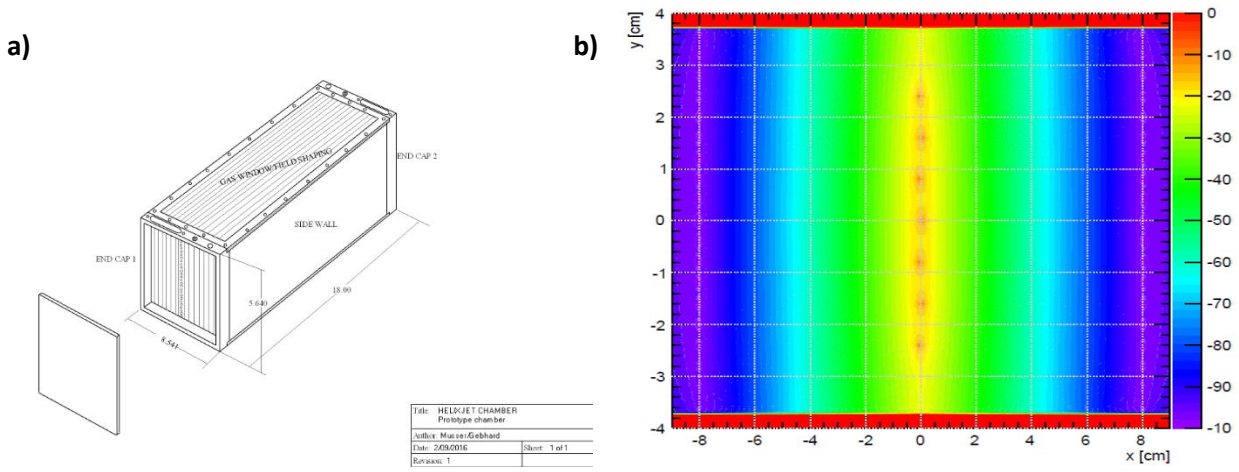

Figure 3.2: a) A sketch of the proto-drift chamber's dimensions. **b)** A heat map of the voltage in a vertical slice of the proto-drift chamber. *Images by Jim Musser.*

Two test runs of the PDCT were run by collaborators at Indiana University. They measured specifically cosmic ray muons, whose mass, charge, and drift velocity in monotonic gas are well known. The PDCT contains a single layer of staggered sense wires, as opposed to the full chamber which will feature layers of the same form. Cosmic ray events were registered by scintillator paddles above and below the PDCT.

Resulting signals are statistically analyzed to find the number of electron clusters dN (proportional to signal strength) to drift time. Electron drift velocity for a given drift time is given by

$$v_{drift} = \frac{ds}{dt} = \frac{ds}{dN}\left(\frac{dN}{dt}\right)$$

If v_{drift} is assumed constant, we may use this time-binned signal distribution, dN/dt, in regions where it is approximately constant, and infer that $\frac{dN}{ds}$ is also approximately constant. For drift times in this region we find the space-time relation,

$$R\left(t_{drift}\right) = t_{drift} \cdot v_{drift} = \frac{ds}{dt} = \frac{ds}{dN}\left(\frac{dN}{dt}\right) \cdot t_{drift}$$

4. Housekeeping Implementation

4.1. Serial Communication

The housekeeping system utilizes serial communication to exchange data and commands from the main board to subsystems. In serial, data is relayed one bit at a time through a transmission bus, as opposed to parallel in which there are multiple simultaneous transmission lines. Specifically, the housekeeping system communicates with subsystems via Universal Asynchronous Receiver/Transmitter (UART) protocol.

4.2. UART

UART protocol is a two bus-wires communication system: each device has a bus for receiving and for transmitting.

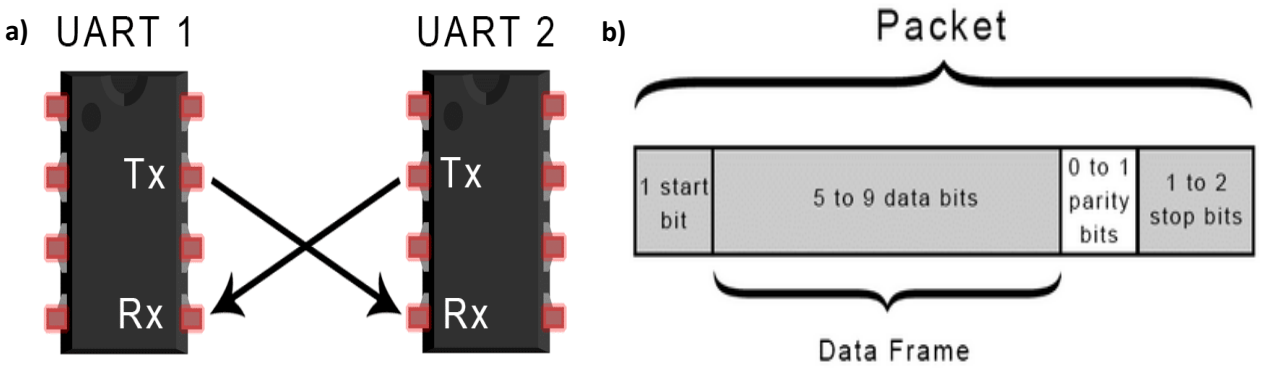

Figure 4.1: a) An example of two connected UART devices. **b)** A typical data block in UART protocol [12].

When transmitting data, there are 3 or 4 'overhead' bits per data block. Overhead is considered bits/bytes that are transmitted but not contained in the original data block. Each data block transferred has attached a 'start' bit to initialize the transfer, an optional 'parity' bit, and 1 or 2 'stop' bit to signal the end of the reading. The parity bit interprets a data block as an integer and is activated only if the integer is even. This way, UART protocol has a way to identify corruption in the transfer of individual bytes of data. Data blocks can take the form of 5-9 bits (here we use 8-bit data blocks for a full byte).

4.3. Hardware

4.3.1. Tiva TM4C-series Launchpad

For testing and implementation, we use the Tiva TM4C123GXL microcontroller as system managers. These boards have been proven to operate well at temperatures HELIX will operate in (-40 - 85°C) [10,11]. Launchpad microcontrollers have a large number of inputs including eight UART, four I2C, and four SPI ports. Though not all inputs may be used simultaneously, as some pins are re-used, all eight UART ports have been tested simultaneously as they will during the experiment.

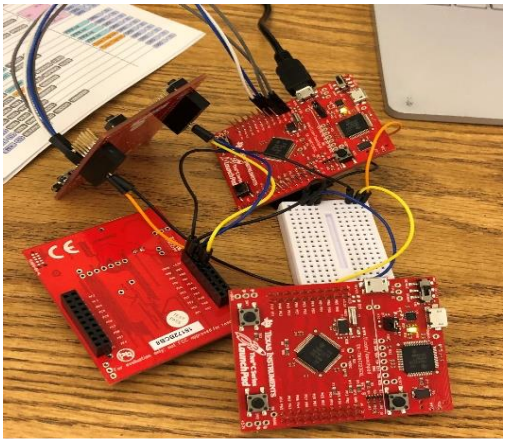

Figure 4.2: Several Tiva C Launchpads connected via serial, creating a mock version of the housekeeping system.

Launchpads proved suitable for testing the system because of their large number of ports and success in past projects, but also because of their built-in micro-USB serial connection, and

an On-board In-circuit Debug Interface (ICDI). I tested each version of the system by flashing software to the microcontroller via USB.

Each serial port on the Launchpad has a corresponding RX (receive) and TX (transfer) pin. By linking launchpads through these ports, I was able to test the housekeeping system with up to three prototype subsystems as in Figure 4.2. This mimics the real housekeeping system hierarchy, shown below.

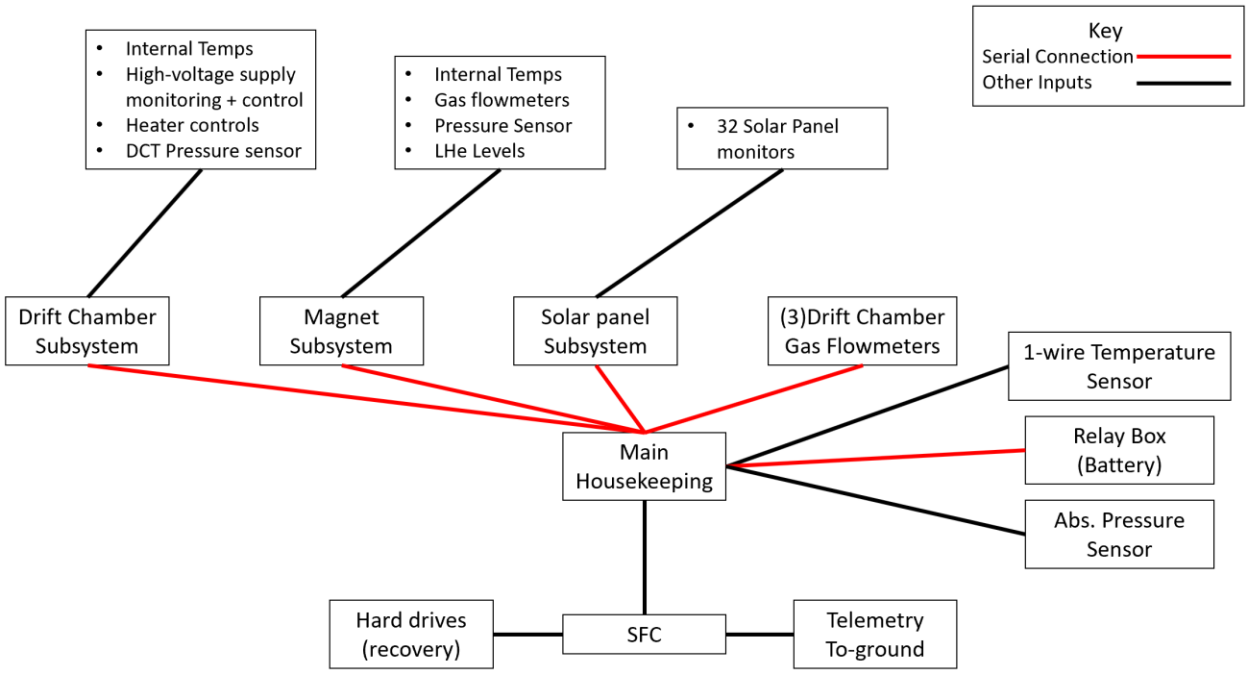

Figure 4.3: The housekeeping hierarchy. Data flows from top to bottom, starting with individual sensors and leading into the main housekeeping board and finally to the SFC.

4.4. Data Packet Structure

Data is sent in 'packets' meant to identify the source, destination, and sensor reading of any communication. Each development board in the housekeeping system has a unique numbered identifier (0-255) that is sent with its transmissions. These ID numbers identify which subsystem the data came from and where it is meant to be sent in the data stream. Information requests are passed alongside a command which instructs the subsystem which sensor to read. That subsystem sends the information back with the same command, and provided with the source ID, the SFC can attribute the message to a specific sensor. All housekeeping commands and data are sent in encoded packets with a standardized header.

Source	Destination	Command	Length (bytes)	Data (0-250 bytes)

The header contains four bytes: the source of the packet, the final destination of the packet, the command identifying the packet's data, and the length of the attached data. The max data length of every packet is 250 bytes.

4.5. Core Functions

Every subsystem in the housekeeping system shares a set of functions vital for consistency in data transmission.

4.5.1. Ping-Pong

A primary internal function the housekeeping system performs on startup is the ability of each subsystem to self-identify. This is useful because all sub-housekeeping systems are plugged in using the same cables – having the option to plug a cable in to any port can help avoid confusion in the system's assembly.

When the main housekeeping board sends the ping-pong command, each subsystem in the data stream will identify itself by responding with the same 'ping-pong' command. The source and destination slots in the header switched. Once this process is completed, the main housekeeping board will store a dictionary of which serial line is connected to which subsystem. Future commands for a subsystem will then only be sent through this serial line. This service was successfully implemented with subsystems in series as well as in parallel, though current plans for the system only require parallel connections to subsystems.

4.5.2. Priority Setting

Periodic sensor readings are taken from each subsystem in three different time periods, linked to the priority levels of low, medium, and high. Each instrument a subsystem measures is hardcoded into its microcontroller. The importance of each measurement is weighted with its priority setting. The housekeeping system provides the utility to change a command/measurement's priority setting on the fly for configuration. The priority system simplifies the data collection process and lessens traffic on the transmission/receiving lines.

4.5.3. Send All

Along the same line of thought as priority setting, the send all command tells a subsystem to take every reading it knows how and send it back. This command is meant to relay a summary of a certain subsystem should an issue arise, or if something otherwise interesting comes up.

4.6. Encoding and Error Detection

Serial communication testing was performed with speeds from 115,000 Hz to 1.5 MHz. Increasing data transmission speeds also increases the likelihood that data is corrupted during the transfer. To guard against faulty data packets, two encoding methods were implemented at the software level.

4.6.1. COBS

To make packets durable against data corruption and errors in transmission, packets are encoded using Consistent Overhead Byte Stuffing (COBS). This encoding method helps identify malformed packets by utilizing a reserved value, the packet delimiter, to discriminate between packets. A perk of using the COBS algorithm bounds the number of extra bytes needed to encode a string of bytes at 2 + int(n/254) (where n is the length of the packet in bytes). Predictable overhead scaling means that the time needed to transfer encoded packets is also predictable.

Given a specific byte as a packet delimiter, typically the '0' byte, COBS transforms a string of bytes in the range [0,255] into the range [0,255] \ {delimiter}, or [1,255]. Inserting the packet delimiter at the end of the string unambiguously signals the end of the transmission, since that byte will not be found anywhere else in the string. The encoding algorithm is as follows:

Specifying a packet delimiter (here '0') and given an arbitrary data string, for example,

0	2	0	0	1

1. Insert first 'overhead' byte: The overhead byte here is the number of bytes until the first special character appears. It is inserted at the beginning of the string:

1	0	2	0	0	1

2. Insert final 'overhead' byte: The packet delimiter should be inserted at the end of the string:

1	0	2	0	0	1	0

3. Replace the first packet delimiter character with the counted number of bytes until the next one appears:

1	2	2	0	0	1	0

4. Repeat step 2 until the sequentially last delimiter remains in the string:

1	2	2	1	1	1	0

If a data packet is corrupted, this delimiter counting mechanism is thrown off, and the likelihood the data stream accidently recovers the pattern before the max data length is transmitted is small. COBS encoding was successfully programmed into the core transmission process of all housekeeping microcontrollers.

4.6.2. Checksum

One last measure is taken to ensure that corrupted data packets will be identified, the checksum. Here, a checksum is an 8-bit addition (or subtraction) of each byte in the data string. This number is added to the end of the data string to be transferred with it. Similar to the parity bit utilized by UART, if the receiving device repeats the addition of each byte received (except the last checksum byte) and the sum does not match, the transmission is identified as faulty. This gives a packet only a 1 in 255 chance of being misinterpreted as uncorrupted.

4.7. Sensor Communication

Testing the solar housekeeping board, in charge of managing the many solar panels on the flight, required the development of an I2C library for facilitating communication.

4.7.1. I2C

I2C protocol, like UART, is a two-bus wire system. However, the buses play different roles: the SDA wire is a serial transmission/receiving bus, and the SCL is a serial clock. The clock functions to set the data transfer rate between devices, whereas in UART the transfer rate must be agreed upon beforehand by both devices. There are two types of devices in I2C: the bus master, which generates the clock, and slaves.

Communication using I2C is more complicated than UART since all communication takes place on one bus. Most devices, like the Tiva C Launchpads, have a standard library of functions which help set up the protocol. Several of these built-in functions include activating pins on the Launchpad for I2C use and performing actions on the transmission line. To simplify solar housekeeping communication code, I created a library of I2C functions which initiates pins for I2C and prepares to send/receive a certain number of bytes. These functions wrap the TM4C functions to initiate the start condition to begin data transfer (from the master bus), setting the slave address of the device being accessed in the outgoing

register, and putting data bytes into the outgoing register. This system was successfully tested with a LTC2992 microcontroller, which controls the experiment's solar panels.

5. Prototype Drift Chamber Analysis

5.1. Drift Chamber Event Recognition

Cosmic rays entering the PDCT triggered scintillator paddles above and below the chamber. Once a paddle was triggered, the PDCT recorded data from sense wires for ~ 1 μs in 1 ns time intervals. In data analysis, the events were registered per wire by finding the 'rising' edge of the voltage signal, if it exists. For example, when sifting through the event data in Figure 5.1, the voltage at time stamp 307 was above a certain voltage threshold, which would be considered the signal's rising edge. Similarly, once the voltage falls below that threshold, we consider the event to be over (the 'falling' edge). Subtracting these two times gives the drift time-above threshold, and the rising edge is considered the drift time.

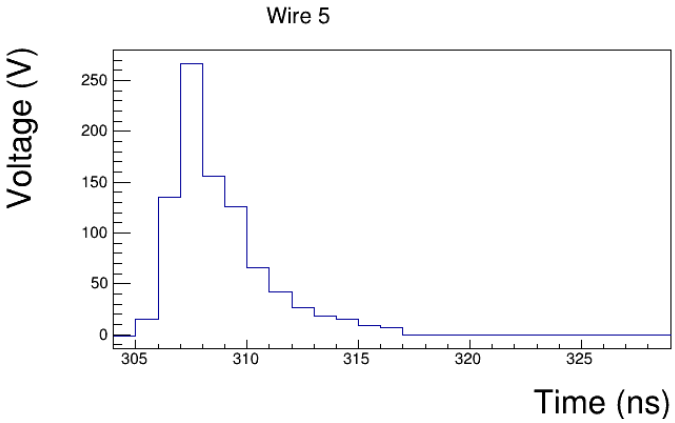

Figure 5.1: A single cosmic ray event registered by one wire.

5.2. Cluster Counting: dN/dt Distribution

Repeating the above process and keeping the drift times for each wire gives the time distribution, dN/dt, as it presents a time-binned fraction of the signal. This distribution represents the proportion of electrons freed in a given drift time.

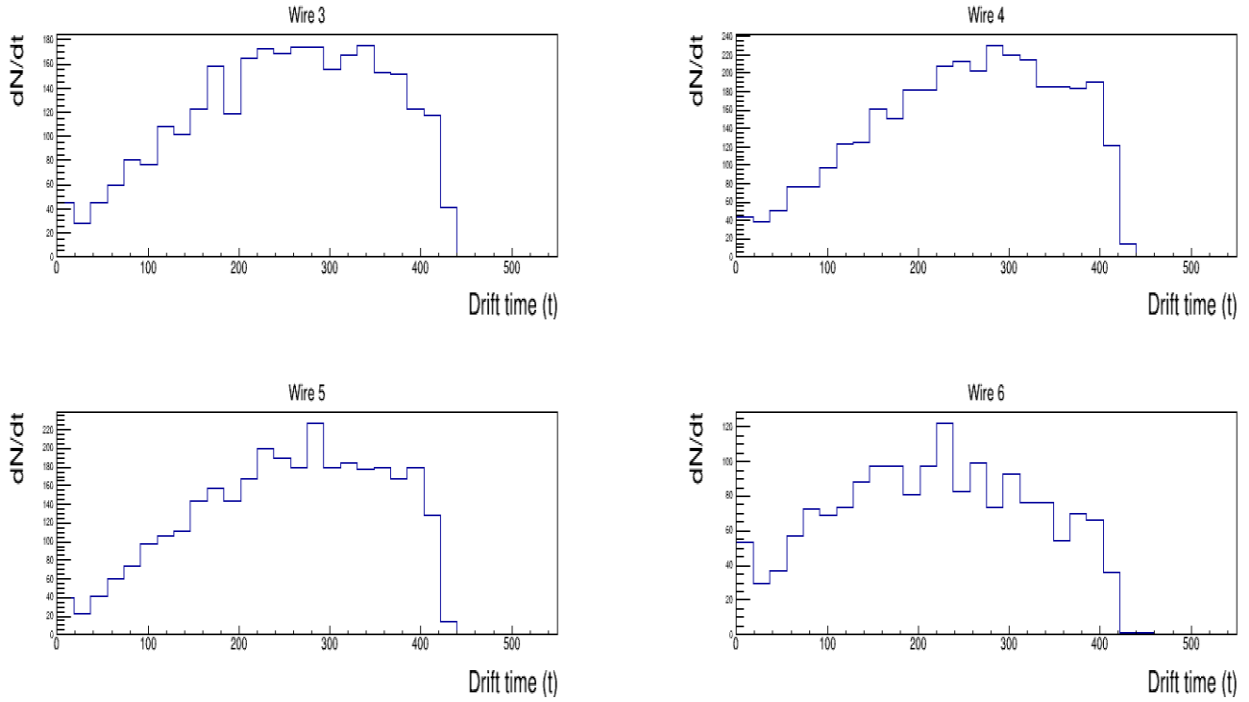

Figure 5.2: Drift time distributions for the middle four wires in the PDCT.

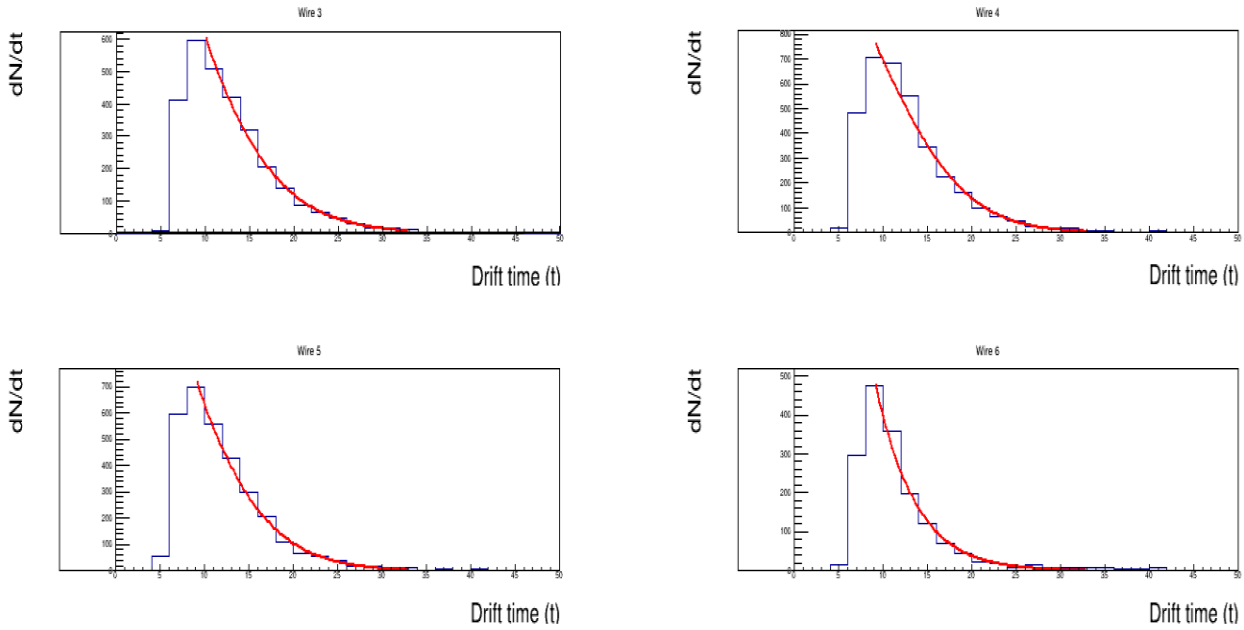

Figure 5.3: Time-over-threshold distributions for the middle four wires in the PDCT. Red lines represent gaussian fits, fit from the peak of the signal to an arbitrary point on the signal's tail.

6. Conclusion

6.1. Summary

The housekeeping system has been tested using my code in data transmission, encoding & error correction, and with its core functions. In the process, several housekeeping systems were integrated and successfully tested with my code, for instance taking two days' worth of data from the magnet sub-housekeeping system.

Prototype drift chamber data was sifted through to begin development of an analysis procedure. Histograms of single events as well as time distributions per wire and per event were created. Fits were performed to time-over-threshold distributions in preparation of later calculations of drift time.

6.2. Future Work

To find a function which gives drift velocity parametrized by radius from the sense wire, we will need to estimate dN/ds by utilizing particle beams. This will give the time-to-distance function, $R(t_{drift})$, from which we can input our drift times and get back its distance from the sense wire. Using these distances, we aim next to reconstruct the path of cosmic rays to get a resolution estimate for a particle's path from the PDCT.

References

[1] Sharma (2008). Atomic And Nuclear Physics. Pearson Education India. p. 478. ISBN 978-81-317-1924- 4.

[2] S. P. Swordy, D. Mueller, P. Meyer, J. L'Heureux, J. M. Grunsfeld, Relative abundances of secondary and primary cosmic rays at high energies, ApJ349 (1990) 625–633. doi:10.1086/168349.

[3] J. J. Engelmann, P. Ferrando, A. Soutoul, P. Goret, E. Juliusson, Charge composition and energy spectra of cosmic-ray nuclei for elements from Be to NI - Results from HEAO-3-C2, A&A233 (1990) 96–111.

[4] H. S. Ahn, P. S. Allison, M. G. Bagliesi, J. J. Beatty, G. Bigongiari, P. J. Boyle, T. J. Brandt, J. T. Childers, N. B. Conklin, S. Coutu, M. A. Duvernois, O. Ganel, J. H. Han, H. J. Hyun, J. A. Jeon, K. C. Kim, J. K. Lee, M. H. Lee, L. Lutz, P. Maestro, A. Malinin, P. S. Marrocchesi, S. A. Minnick, S. I. Mognet, S. Nam, S. L. Nutter, I. H. Park, N. H. Park, E. S. Seo, R. Sina, S. P. Swordy, S. P. Wakely, J. Wu, J. Yang, Y. S. Yoon, R. Zei, S. Y. Zinn, Measurements of cosmic-ray secondary nuclei at high energies with the first flight of the CREAM balloon-borne experiment, Astroparticle Physics 30 (2008) 133–141. arXiv:0808.1718, doi:10.1016/j.astropartphys.2008.07.010.

[5] Obermeier, M. Ave, P. Boyle, C. Höppner, J. Hörandel, D. Mueller, Energy Spectra of Primary and Secondary Cosmic-Ray Nuclei Measured with TRACER, ApJ742 (2011) 14. arXiv:1108.4838, doi:10.1088/0004-637X/742/1/14.

[6] T. Hams, L. M. Barbier, M. Bremerich, E. R. Christian, G. A. de Nolfo, S. Geier, H. Gobel, S. K. Gupta, M. Hof, W. Menn, R. A. Mewaldt, J. W. Mitchell, S. M. Schindler, M. Simon, R. E. Streitmatter, Measurement of the Abundance of Radioactive ^{10}Be and Other Light Isotopes in Cosmic Radiation up to 2 GeV Nucleon^{-1} with the Balloon-borne Instrument ISOMAX, ApJ611 (2004) 892–905. doi:10.1086/422384.

[7] M. Simon, Test of the Diffusion Halo and the Leaky Box Model by means of secondary radioactive Cosmic Ray Nuclei with different life times, International Cosmic Ray Conference 4 (1999) 211.

[8] Putze, L. Derome, D. Maurin, A Markov Chain Monte Carlo technique to sample transport and source parameters of Galactic cosmic rays. II. Results for the diffusion model combining B/C and radioactive nuclei, A&A516 (2010) A66. arXiv:1001.0551, doi:10.1051/0004-6361/201014010.

[9] W. Blum, W. Riegler, and L. Rolandi, Particle Detection with Drift Chambers (Springer, Berlin, 2010).

[10] Texas Instruments, "Tiva™TM4C123GH6PM Microcontroller," DS-TM4C123GH6PM datasheet, 2014.

[11] Circuit Basics. n.d. Basics of UART Communication. [online] Available at: <https://www.circuitbasics.com/basics-uart-communication/> [Accessed 1 April 2020].

[12] Chefdeville, Maximilien & Schmitz, Jurriaan & Colas, Paul & Graaf, Harry. (2009). Development of micromegas-like gaseous detectors using a pixel readout chip as collecting anode.

[13] M. E. Wiedenbeck, D. E. Greiner, A cosmic-ray age based on the abundance of Be-10, ApJ239 (1980) L139–L142. doi:10.1086/183310.
[14] J. A. Simpson, M. Garcia-Munoz, Cosmic-ray lifetime in the Galaxy - Experimental results and models, Space Sci. Rev.46 (1988) 205–224. doi:10.1007/BF00212240.
[15] N. E. Yanasak, M. E.Wiedenbeck, R. A. Mewaldt, A. J. Davis, A. C. Cummings, J. S. George, R. A. Leske, E. C. Stone, E. R. Christian, T. T. von Rosenvinge,W. R. Binns, P. L. Hink, M. H. Israel, Measurement of the Secondary Radionuclides ^{10}Be, ^{26}Al, ^{36}Cl, ^{54}Mn, and ^{14}C and Implications for the Galactic Cosmic-Ray Age, ApJ563 (2001) 768–792. doi:10.1086/323842.